

Effective supervisory controller to extend optimal energy management in hybrid wind turbine under energy and reliability constraints

Billel Meghni¹ · Djalel Dib² · Ahmad Taher Azar^{3,5} · Abdallah Saadoun⁴

Received: 8 September 2016 / Revised: 5 December 2016 / Accepted: 15 December 2016 / Published online: 2 January 2017
© Springer-Verlag Berlin Heidelberg 2016

Abstract One of the major factors that can increase the efficiency of wind turbines (WTs) is the simultaneous control of the different parts in several operating area. The main problem associated with control design in wind generator is the presence of asymmetric in the dynamic model of the system, which makes a generic supervisory control scheme for the power management of WT complicated. Consequently, supervisory controller can be utilized as the main building block of a wind farm controller (offshore), which meets the grid code requirements and can increase the efficiency and protection of WTs in (region II and III) at the same time. This paper proposes a new effective adaptive supervisory controller for the optimal management and protection simultaneously of a hybrid WT, in both regions (II and III). To this end, the second order sliding mode with the adaptive gain super-twisting control law and fuzzy logic control are used

in the machine side, batteries side and grid side converters, to achieve four control objectives: (1) control of the rotor speed to track the optimal value; (2) adaptive control (commutative mode) in order to maximum power point tracking (MPPT) or power limit in various regions; (3) regulate the average DC link voltage near to its nominal value; (4) ensure: a smooth regulation with high quality of power supply injected into the grid, a satisfactory power factor correction and a high harmonic performance in relation to the AC source and eliminating the chattering effect. Results of extensive simulation studies prove that the proposed supervisory control system guarantees to track reference signals with a high harmonic performance despite external disturbance uncertainties.

Keywords Supervisory control · Optimal management · FLC · Adaptive control · Super-twisting control · Power limit

✉ Ahmad Taher Azar
ahmad_t_azar@ieee.org; ahmad.azar@fci.bu.edu.eg

Billel Meghni
maghni_1990@yahoo.fr

Djalel Dib
dibdjal@gmail.com

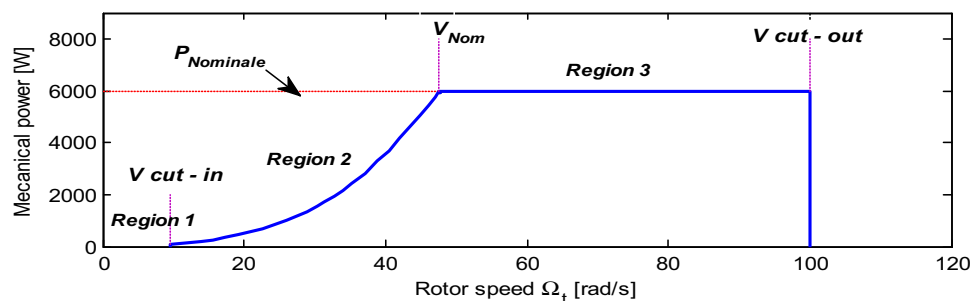
Abdallah Saadoun
saadoun_a@yahoo.fr

- ¹ Department of Electrical Engineering, Faculty of Applied Science, University of Kasdi Merbah, 3000 Ouargla, Algeria
- ² Electrical Engineering Department, University LarbiTebessi, Tebessa, Algeria
- ³ Faculty of Computers and Information, Benha University, Banha, Al Qalyubiyah, Egypt
- ⁴ Department of Electronics, University of Badji Mokhtar, Annaba, Algeria
- ⁵ Nanoelectronics Integrated Systems Center (NISC), Nile University, Cairo, Egypt

1 Introduction

Because of the environmental problems, the oil crisis and the growing demand for alternative sources of energy, wind power is the greatest mature of the different renewable energy technologies which received a lot of concern and attention in perceptible many parts of the world [1]. Nowadays, specifically related to offshore WTs, a new aspect in the construction and a mode of operation demonstrate in wind conversion technology. Currently most WTs operate at variable speed without gearbox and based on permanent magnet synchronous generator (PMSG), this type can work with: a good performance, high reliability, a great ability to track and the extract the maximum power in each wind speed, require a simple maintenance and less expensive than gearbox technology [2–4].

Fig. 1 Operation regions for variable speed wind turbine (VSWT)



Practically and for safety reasons turbines and uniform stability between supply and demand of energy, WT's operate in a well-defined range of wind speeds bounded by (V_{min})(cut-in) and (V_{out}) (cut-out) as is shown in Fig. 1, where the possibility of four different operating zones [5].

Within these limits and to protect the PMSG, the WT system is sized to provide a power rating P_{Nomile} at a wind speed of V_{Nom} . Consequently, four main operating areas can be distinguished: The region (I) is the starting region of the generator, it begins when the wind speed exceeds (V_{cut-in}). The region (II): when the wind speed exceeds (V_{cut-in}), a control algorithm for extracting the maximum power from the wind has been applied, where the blade pitch angle was held constant at its value minimum $\beta = 0$. The region (III) is defined when the wind speed exceeds V_{Nom} but in wind speed ($V_{cut-out}$), the turbine works at a fixed speed to produce a constant power equal to the nominal power of PMSG. In the last region (region IV), the blades of the turbine are carried flags ($\beta = 90$) to protect the wind [5,6].

Despite this characteristic, wind force, it is highly fluctuating (also called volatile) for this reason the utmost challenging of the wind energy is the intermittent and unpredictable nature, Which makes the WT's integration in grid very difficult, causing a deterioration in the quality of electrical power [7]. Therefore, the WT manufacturers are supporting these turbines with different energy storage systems, in order to keep the power grid operating safely and reliably, balancing the offer and demand grid side [8,9]. However, practically and concerning the WT's at variable speed, these advantages remain limited and inadequate. Therefore, effective architecture of control systems are one of the major issues in hybrid VSWT (to extract maximum wind power within the limits to protect the WT system in the region III and to achieve load demand variation and load management), to prevent possible deterioration on the quality of electrical power injected in the grid, where variations of the loads and generations are significant in the system.

It considers all these obstacles and various constraints one of the most motivations for the researchers in this field to optimize and develop on effective and robust control manner for WT's. For instance, in the last years the MPPT techniques for

wind energy systems has been optimized in many literatures [5], to track the MPPs in region(II) under fluctuating wind speed (a wind gust). Some of these techniques include: hill-climb searching (HCS)[5], sliding mode control (SMC)[10], perturb and observe (P&O) [5], FLC techniques [11] and tip speed ratio (TSR) [5]. Several methods of power limitation control and pitch power control have been advanced in some studies [12–14]. In the same context a novel methods to control the mechanical speed of the PMSG/WT have been designed in many papers in order to obtain the optimum system efficiency (MPP). Some of these techniques are first order sliding mode control (FOSMC) [15], SOSMC [16], FLC [17] and robust control [18]. As previously mentioned, numerous manufacturers of VAWTs [9] advanced the performance benefits of adding energy storage systems in WT, to reduce the variable and relatively unpredictable and random nature of wind energy, ensuring more performance and easily management between generations and demand powers whatever the wind speed, in order to ensure the safety and quality of electricity supply in the grid. More recently and on the subject of the electrical energy quality exchanged between the PMSG and the grid, modern control strategies based on the robustness, efficiency and reliability have been designed and implemented for large wind farm technologies to smooth power flow regulation (grid active and reactive powers) such as: FLC [19–21], robust control [22]and SMC [23–25].

Based on our previous research experience on WT hybrid power system with battery storage and their supervisory control system [26], this paper provides a key contribution is to define a detailed model based on offshore WT with a storage system (battery) and to propose their novel supervisory control system to maximize and improve the extracted, delivered (grid) powers quality and protecting all the system. This novelty (proposition) is based on the combination and application of the reliable, efficient and robust design techniques used in the wind system technology to make it work as a complementary in various conditions, in order to create a best hybrid WT's (it gives us competition in the commercial market).

Furthermore, contrary to the works found in the literature (recent), this work presents a new approach to control

and management for extended control of hybrid VSWT that includes simultaneously the two operating regions (II and III). This adaptation (commutation of control system in both regions) may provide better performance in all possible operational scenarios of the wind (ensure the continuity of power production in a wide range of wind speeds conditions): exploiting and extracting the maximum power from the wind, storage of excess power, compensation of power between supply and demand, limiting the upper power at nominal generator or demand. To reach this goal, three power converters are controlled in a complementary manner; the first is the rectifier (AC/DC) generator side, the second is the (DC–DC) converter which links (DC link voltage and storage battery) and the last is the inverter (DC/AC).

This paper is organized as follows. In the Sect. 2, a view of the previous related work is described. Section 3, presents (WT, PMSG and energy storage system (ESS) mechanical and electrical modelling. In Sect. 4, the proposed control system designed in this study is detailed precisely. While in Sect. 5, numerical results (simulation) are illustrated. Finally, the conclusions and future work are provided in the final section.

2 Related work

The electric power generated by VSWTs is considered one of the most important topics that has long fascinated many scientists aims to improve the monitoring system performance (VSWT) and to ensure a better quality of extract and power delivered to the grid (where we find several advanced control techniques that include various modes). Such as artificial neural networks (ANN) [27–29], FLC [30–32], FOSMC [15, 33, 34] and SOSMC [35–37]. The main objective for this interest is that these methods (algorithms) and structures have mainly focused on how to optimize, maximize and extending the use of wind energy. However, the modern study stayed inadequate because of multiple ignored or neglected issues such as: power flow control, MPPT control, speed control, power limit control and energy storage system. One of these problems contributes to driving performance deterioration of WT system. In Ref. [38], the authors use a PSIM software integration with Matlab/Simulink, also the FLC based MPPT algorithm was performed, in this work the results are limited, the general construction of the WT system is very simple without a storage system, power limitation system (security system) and without effective grid side control (grid power). Moreover, in the Ref. [39], a technique has been proposed based on the strategy FOSMC to achieve grid power flow control. The results show the presence of the chattering phenomenon in the both active and reactive power that means a poor power quality produced by the WT system injected in the grid. Furthermore, in Ref. [3],

the author presents a new MPPT algorithm applied to a small WT based on PMSG. On the other hand the operating range of this system is limited in the region (II), because it not contains any limit power control or pitch control in high wind speed. On [9, 40–42] the authors modeled and controlled based on a VSWT asynchronous doubly fed generator (DFIG), this system is supported by an energy storage system. Simulation results in different operating modes are convincing but they remain insufficient. In these studies, we observed a complete lack advanced control techniques (effective and robust) in the vital points of the VSWT as MPPT and control of energy flow, which has a lower yield with a poor quality the power injected to the grid. In addition, these WTs are low only in a stable state of operation (no fault in the grid and no wind speed burst). Also in these studies, the authors adopted only on the operating area 2 (this is what makes activity limited by WT). The simulation results in [11] are good and motivating, where the author controlled the wind system by applying advanced control techniques such FLC and SOSMC while applying a method of power limitation. The contributions in this study are limited because of: (1) the choice of the machine used in this system is inappropriate. (2) The author has ignored the use of a storage system to take advantage of excess wind energy (this increases the efficiency of wind with expanding the operating range of the latter (several lines power). Finally the author did not provide any assessment, comparison and analysis harmonic to prove their technical control applied (SOSMC). In the Refs. [43–46], the authors have designed new MPPT algorithms to extract and improve the maximum power of wind (region II). Due to a most contributions, these fields (MPPT) have brought a many achievements and success especially in recent years. These accomplishments are limited and inadequate to protect the WTs in different regions. In addition, these algorithms (MPPT) are not able to supply the demand all the time (if the power demand exceeds the power of the wind), and the storage system is essential to compensate for lack of power supplied to consumer. In Ref. [26] the authors generally succeed in the choice of the supervisory control system which applied in hybrid VSWT. But they are neglect the protection of the wind system (electric and mechanic) under high wind speed in addition they are limiting the operating range of WT.

Among the studies and the results reported in the literature, they remain incomplete for many reasons:

- The multiplicity of obstacles and problems facing it.
- Partial and separate optimization in some points of the WTs.
- Diversity in construction of wind turbines.
- The difficulty and complexity of integrating wind turbines in grid.

Among the proposed solutions, the new surveillance monitoring system we have proposed is considered a universal solution (in VSWT systems).

Nomenclature

V_{sd}, V_{sq}	d, q -axis stator “PMSG” currents
I_{sd}, I_{sq}	d, q -axis stator “PMSG” voltage
R_s, L_d, L_q	Stator resistance, d, q -axis PMSG inductance components respectively
ψ_m	The magnetic flux
T_e	The machine torque
ω_e	The electric pulsation of PMSG
D_T	The damping coefficient
J_T	The mass moment of inertia
n_p	The number of pole pairs
$I_{avg} (A)$	The mean discharge current
Q_e	The battery’s capacity
WECS	The wind energy conversion system
$E_{batdisch}, E_{batcharg}$	Respectively are battery discharge and charge voltage
R_i	The battery resistance
Q	The battery capacity
i_t, i^*	Respectively are battery charge and filtered current
V_{di}, V_{qi}	The inverter voltages components
R_g, L_{dg}, L_{qg}	Respectively are resistance and d, q -axis grid inductance
V_{bat}, E_0	Respectively are battery rated voltage and the internal EMF
$V_{dg}, V_{qg}, I_{dg}, I_{qg}$	Respectively are d, q -axis grid voltage and currents
$C (A \cdot s)$	The battery’s charge
DOC	The battery depth of charge

3 Wind turbine modeling

The WT topology used in this study is constituted: a VSWT “horizontal axis turbine with a three-bladed rotor design” directly coupled to PMSG shaft (without a gearbox) as shown in Fig. 2. This system is supported by the energy storage system (a lead acid battery) associated with DC-link bus voltage with a DC–DC converter.

3.1 Turbine model

The aerodynamic power P_t available on the shaft of the turbine is expressed by Azar and Zhu [10]:

$$P_t = \frac{1}{2} \rho \pi R_t^2 v^3 C_p (\lambda, \beta) \tag{1}$$

where v is the wind speed, ρ is the air density.

The C_p (power coefficient) represents the aerodynamic efficiency of the WT is dependent on tip speed ratio (TSR) “ λ ” and the orientation angle of the blade β , it defined as [47]:

$$C_p = 0.073 \left(\frac{151}{\lambda_i} - 0.058\beta - 0.002\beta^{2.14} - 13.2 \right) e^{\frac{-18.4}{\lambda_i}} \tag{2}$$

$$\text{where } \lambda_i = \frac{1}{\frac{1}{\lambda - 0.02\beta} - \frac{0.003}{\beta^2 + 1}}$$

The speed ratio is expressed as the ratio between the linear speed of the blades and the wind speed:

$$\lambda = \frac{R_t \Omega_t}{v} \tag{3}$$

or Ω_t is the speed of the PMSG/turbine, R_t represents the radius of rotor.

3.2 PMSG model

The stator voltages equations of the PMSG are described in the Park d, q axis (synchronous reference frame) as following [47]:

$$\begin{cases} V_{sd} = R_s I_{sd} + L_d \frac{dI_{sd}}{dt} - \omega_e L_q I_{sq} \\ V_{sq} = R_s I_{sq} + L_q \frac{dI_{sq}}{dt} + \omega_e (L_d I_{sd} + \psi_m) \end{cases} \tag{4}$$

The expression of the electromagnetic torque is obtained as [48]:

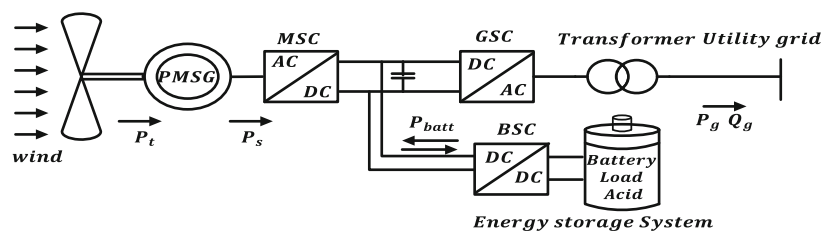
$$T_e = \frac{3}{2} n_p (\psi_m I_{sq} + (L_d - L_q) I_{sd} I_{sq}) \tag{5}$$

3.3 The energy storage system ESS model

Currently, lead acid batteries are most commonly used for WT applications. The mathematical model given by Eq. (1) describes the simplest physical system in [49] that simulates the behavior of the battery and its voltage:

$$V_{bat} = E_{bat} - R_i i \tag{6}$$

Fig. 2 Wind generation system configuration



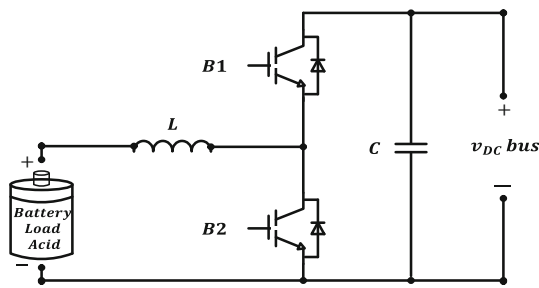


Fig. 3 Schematic circuit of the battery power converter

For the period of the discharging or charging of the battery, the expression of the battery load voltage is established in rated value as [40]:

$$\begin{cases} E_{batdisch} = E_0 - K \frac{Q}{Q-i_t} i^* - K \frac{Q}{Q-i_t} i_t + f_{hyst-disch}(i) \\ E_{batcharg} = E_0 - K \frac{Q}{0.1Q+|i_t|} i^* - K \frac{Q}{Q-i_t} i_t + f_{hyst-char}(i) \end{cases} \quad (7)$$

The instantaneous value of the state of charge (SOC) is determined by Sarrias et al. [40]:

$$SOC = 1 - \frac{Q_e}{C(0, \theta)}, \quad DOC = 1 - \frac{Q_e}{C(I_{avg}, \theta)} \quad (8)$$

3.4 The battery converter model

The DC–DC bidirectional converter is widely used in the storage battery connections with renewable energy systems (wind energy). Regardless of the variation of the battery voltage during operating conditions, the converter is used to adjust the DC voltage bus at a desired nominal value. It is composed of an inductor and two (IGBT) insulated gate bipolar transistor of diode switches to combine two operating modes [7] as shown in Fig. 3.

- In the first mode, the converter operates as a unidirectional buck when switches (B1 switch and diode B2) are closed during this period (the loading phase) DC bus provides active power to the BESS.
- In the second mode, the converter operates as a unidirectional lift to ensure the discharge of the battery in the DC bus and via B2 switch and diode B2.

4 Proposed control system

In hybrid/ WT technology and in order to overcome the various constraints (fluctuations in electricity supply and demand, sporadic nature of the wind in different operating areas and the unexpected faults in the system and grid), we

need to establish and application a comprehensive and effective supervisory control system. This control system is able to provide several goals, product stability, security and optimize the extracted power in multiple regions (II and III). This novel control is based on optimizing of our concept of classical supervisory control [22].

The major objective most of the control systems used in this work are:

- *In region II* Optimizing power extracted from the wind by the combination achieved between the (FLC/SOMSC) and implemented to machine side converter (MSC).
- *In region III* Maintaining the extracted power close to its nominal value ($V > V_{Nom}$), through adaptive control (FLC–SOSMC–MPPT and the detected extracted power as a feedback).
- *In both regions (II and III)* Managing energy between «extracted wind power, power grid demand and battery stored power», using the effective supervisory controller “switching algorithm» through the battery side converter BSC.
- *In both regions (II and III)* Improvement of the electric power quality for grid, through the new efficiency and robust strategy control based on (DPC–SVM–SOSMC) and implemented in the grid side converter (GSC).

4.1 Control of the machine side converter (MSC)

VSWT allow extracting a maximum power for each wind speed. However, this degree of freedom requires a system of speed /sophisticated and robust power control to protect both the “PMSG/WT” system and to monitor the point of maximum available power (region II) and to stabilize the captured power at nominal value when the wind speed exceeds has some value by (region III). In this section, we showed the design of the MSC as shown in Fig. 4, that includes two additional operating modes (adaptive).

4.1.1 Tracking mode (region II)

In this area and to meet the total demand for power, the turbine operates at variable speed under a nominal wind speed between (V_{cut-in}) and (V_{Nom}). For this goal we have created two control loops with cascade control structure. In the outer loop, a novel algorithm basedMPPT has been suggested (FLC–SOSMC) to permanently obtained amaximum power (aerodynamic energy). The inner loop allows controlling the rotation speed of the PMSG via a (FOC) strategy which has been designed for controlling d, q -axis current of the PMSG [50]. As shown in Fig. 5, for an instantaneous variation of the wind speed and for $\beta = 0$, the FLC–SOSMC based (MPPT) algorithm generates the q -axis current component that opti-

Fig. 4 MSC control strategy

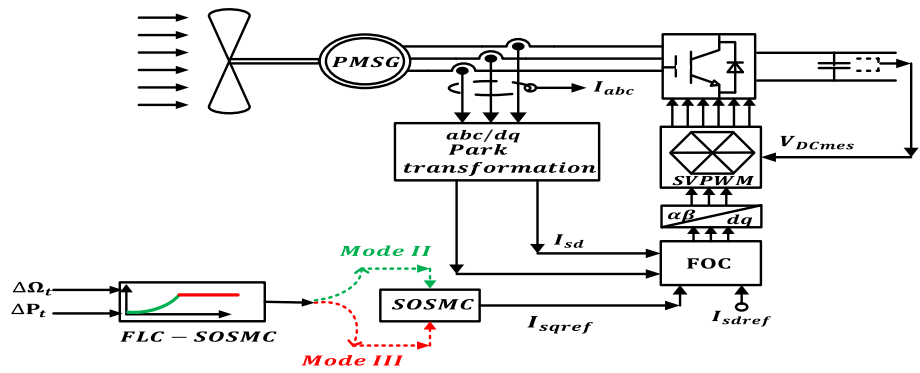


Fig. 5 Real tracking of the optimal rotational speed ORC in regions “II and III”

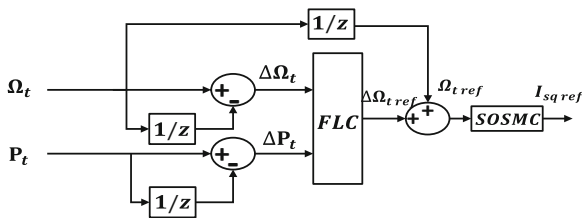
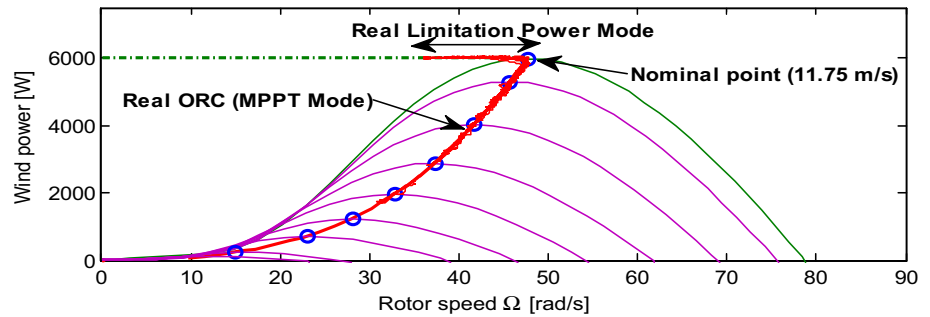


Fig. 6 Block diagram of FLC-MPPT

mize the rotation speed of the PMSG to extract power from the turbine.

In the absence of any information about the “characteristic, parameter” of the WT and without the wind sensor, the FLC method ensures a smooth, reliable and quick tracking of the MPP. Besides that this algorithm is used for generating an optimal reference at each wind speed as shown in Fig. 6.

The FLC-MPPT method is one of the best performing control technique in this domain (wind energy) because it is popular and universal for the various WT systems [11]. The suggested FLC-MPPT is appears in Fig. 6, it consists: two inputs (power and rotational speed variation ΔP_t , $\Delta \Omega_t$ respectively) and the output variable (one) is the change in (Ω_{tref}). The formation of the fuzzy rules of the system is given in Table 1. The Eq. (9), show a linear relationship between the mechanical power “extracted”, wind speed and the optimum speed rotation.

Table 1 Fuzzy rule table

$\Delta \Omega_t$	ΔP_t								
	NBB	NB	NM	NS	ZE	PS	PM	PB	PBB
N	PBB	PB	PM	PS	ZE	NS	NM	NB	NBB
ZE	NB	NB	NM	NS	ZE	PS	PM	PB	PB
P	NBB	NM	NS	NB	ZE	PM	PM	PM	PBB

$$\begin{cases} \Delta P_t = P_t(k) - P_t(k - 1) \\ \Delta \Omega_t = \Omega_t(k) - \Omega_t(k - 1) \\ \Omega_{tref} = \Omega_t(k - 1) + \Delta \Omega_{tref} \end{cases} \quad (9)$$

In the same part, as shown in Fig. 6, the reference speed generated (imposing) by MPPT controller, this reference speed is used as an input to the speed control loop to create the q-axis PMSG current component. Therefore, to assure this regulation (optimal speed of PMSG), a new SOSMC algorithm has been proposed and designed. In this algorithm, the chattering phenomenon can be removed to give a smooth trajectory tracking compared with conventional FOSMC.

The speed Ω_t sliding surface is taken as follows:

$$s_{\Omega_t} = \Omega_{tref} - \Omega_t \quad (10)$$

Then we have:

$$\dot{s}_{\Omega_t} = \dot{\Omega}_{tref} - \dot{\Omega}_t = \dot{\Omega}_{tref} - \frac{1}{J} (T_t + T_e - F \Omega_t)$$

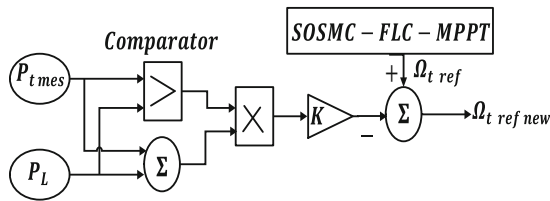


Fig. 7 Detailed block diagram of the PowerLimit

If we put G_{Ω_t} as follows:

$$G_{\Omega_t} = \dot{\Omega}_{tref} - \frac{1}{J} (T_t - F \Omega_t) \quad \text{Thus: } \ddot{s}_{\Omega_t} = \dot{G}_{\Omega_t} - \frac{\dot{T}_e}{J}$$

The SOSMC proposed in this part is comprises two parts based on super twisting algorithm (ST) as mentioned in [51].

$$I_{sqref} = I_{sqeq} + I_{sqN} \quad \text{Where: } I_{sqN} = I_1 + I_2$$

$$\text{With: } \begin{cases} I_1 = -N_1 \text{sign}(s_{\Omega_t}) \\ I_2 = N_2 \sqrt{|s_{\Omega_t}|} \text{sign}(s_{\Omega_t}) \end{cases}$$

The constants N_1 and N_2 are chosen in a manner to assure in finite time the convergence of the sliding manifolds as follows [52]:

$$\begin{cases} N_1 > \frac{\mu_i}{L_g} \\ N_2 \geq \frac{\mu_i(k_i + \mu_i)}{L_g^2(k_i - \mu_i)} \end{cases} \quad (11)$$

4.1.2 Power limit (region III)

To provide greater freedom of operating in VSWT accompanied by a permanent protection, the power limiting system is inevitable (above the nominal wind speed of 11.75 m/s, as shown in the control (Fig. 5). This system intervenes except in region III “in the tolerable beach between P_t and $1.2 P_t$ ” to ensure a limitation of the extracted power (stable operation mode) to protect the WT and PMSG. The control circuit shown in Fig. 7, is added to the previous design “SOSMC-FLC-MPPT” to generate a reduced reference speed during the period of increase of the extracted power (to prevent the continuation of producing quantities of high power). The new reference rate $\Omega_{trefnew}$ is achieved by reducing the amount K of early speed [53] as shown in:

$$\Omega_{trefnew} = \Omega_{tref} - \Delta \Omega_t \quad (12)$$

4.2 Control of the battery (ESS) side converter (BSC)

In order to ensure the stability of the bus voltage to 800 V in all work scenarios, a DC/DC converter is implemented and controlled. This converter is influenced by changes of

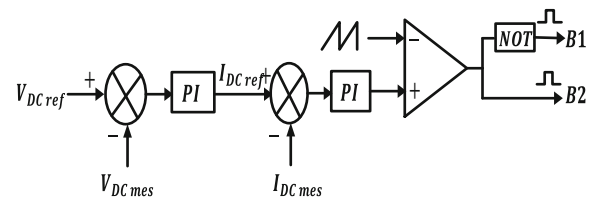


Fig. 8 A control diagram for battery side converter (BSC)

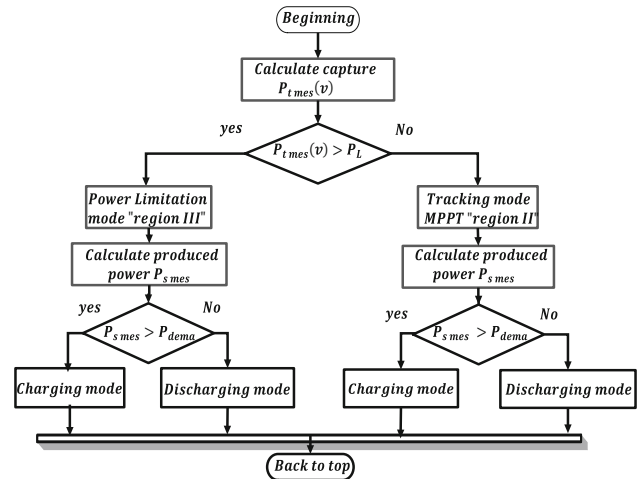


Fig. 9 Flowchart of the charges or discharges cycle in the battery (ESS) side converter

voltage (caused by the variation of the production and the demand) that causes a reduction or increase of the voltage in the battery ESS and DC-link voltage.

In Fig. 8, we showed two cascade control loops that provide bidirectional power. The outer loop is used to compare the two voltages (measurement and reference) at the DC-link bus. This regulation helps maintain the bus voltage to a nominal value at the end to generate a reference current to the input of the internal control loop. The latter supplies control signals to the converter which adjusts the charge and discharge cycles of the storage system via the cyclical ratio [54].

The algorithm presented below Fig. 9, describes excessively various operating modes (charging and discharging of the battery) in nominal and instantaneous variations of the following variables (wind speed, rated power, extracted power and the supply/demand grid power).

The following criteria are the basis of this algorithm:

- If the power captured by the WT are less than the nominal power of the turbine can select the operating region of the turbine/PMSG by MPPT. In the same situation, the extracted power from the wind speed is compared with the power specified by the demand: this means the way of power between the battery and the PMSG.
- Otherwise, if the speed exceeds the nominal wind, the operating area of the turbine is moved to the region III, mode 2 (power limitation) and therefore the power

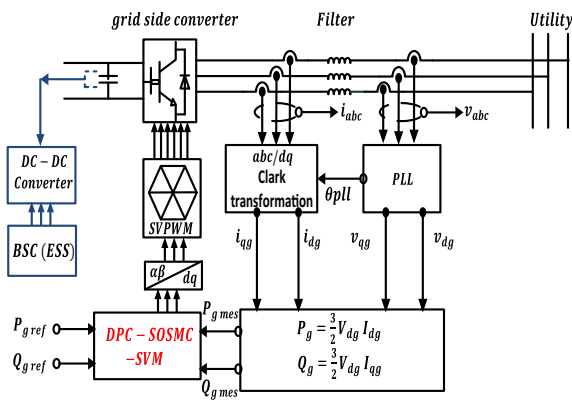


Fig. 10 A control diagram for GSC used “DPC–SVM based on SOSMC”

produced to be always constant where the load and the system of discharge V_{DC} are imposed by the amount of power required at the electrical grid.

4.3 Control of the grid side converter (GSC)

This converter allows you to: control the exchange of the active and reactive power between the PMSG and the grid. Ensure constant power to the user in case of grid faults or wind power changes to maintain DC-link voltage constant. To achieve these objectives, we have proposed a new approach of direct power control (DPC) which is based on an algorithm SOSMC and supported by the SVM technique.

Figure 10, shows the GSC circuit diagram regardless of the continuous bus control (which is used a bi-directional DC/DC converter). In this case, a single control loop is implemented (inner loop), which comprises an active and reactive power control on the basis of non-linear regulator SOSMC. The approach of the DPC–SOSMC–SVM strategy directly generates the reference voltage unlike the conventional method of vector [39].

In the control of nonlinear systems or having non-constant parameters, the conventional control laws [55,56] may be insufficient. For this reason, we must use effective and robust control techniques such as [10,57–68] that are “insensitive to parameter variations, to disturbance and nonlinearities”. In the literature, the sliding mode control is considered one of the most important of these techniques [11,25,26,34–36]. The switching high frequencies (chattering) induced by the latter is the main disadvantage to the practical implementation of this method. To reduce this phenomenon (chattering), a higher order control by sliding mode based on nth derivate must be used to keep the same characteristics of the original technical (robustness, efficiency and speed) [69].

In reference frame rotating synchronously and to ensure the active and reactive grid power control, the electrical

power equations P_g, Q_g are linked to the grid currents as follows [38]:

$$\begin{cases} P_g = \frac{3}{2} V_{dg} I_{dg} \\ Q_g = \frac{3}{2} V_{dq} I_{qg} \end{cases} \quad (13)$$

The optimal reactive power is set to zero to ensure a unity power factor operation of this system: $Q_{gref} = 0$ whereas the optimal active power P_{gref} can be written depending on the needs of the grid.

The sliding surface for the p_g, Q_g powers is shown:

$$\begin{cases} s_P = P_{gref} - P_g \\ s_Q = Q_{gref} - Q_g \end{cases} \quad (14)$$

The first derivatives of the surfaces s_P, s_Q are represented:

$$\begin{cases} \dot{s}_P = \dot{P}_{gref} - \frac{1.5V_{dg}}{L_g} (-V_{dg} - R_g I_{dg} + L_g \omega_g I_{qg}) - \frac{V_{id}}{L_g} \\ \dot{s}_Q = \dot{Q}_{gref} - \frac{1.5V_{qg}}{L_g} (-V_{qg} - R_g I_{qg} - L_g \omega_g I_{dg}) - \frac{V_{iq}}{L_g} \end{cases} \quad (15)$$

If we put G_P and G_Q as follows:

$$\begin{cases} G_P = \dot{P}_{gref} - \frac{1.5V_{dg}}{L_g} (-V_{dg} - R_g I_{dg} + L_g \omega_g I_{qg}) \\ G_Q = \dot{Q}_{gref} - \frac{1.5V_{qg}}{L_g} (-V_{qg} - R_g I_{qg} - L_g \omega_g I_{dg}) \end{cases} \quad (16)$$

The second derivation of s_P, s_Q are displayed:

$$\begin{cases} \ddot{s}_P = \dot{G}_P - \frac{\dot{V}_{id}}{L_g} \\ \ddot{s}_Q = \dot{G}_Q - \frac{\dot{V}_{iq}}{L_g} \end{cases} \quad (17)$$

The SOSMC proposed in this part is comprises two parts based on ST algorithm as mentioned in [51].

Where $\begin{cases} V_P^{ref} = V_P^N + V_P^{eq} \\ V_P^N = w_1 + w_2 \end{cases}$

With $\begin{cases} \dot{w}_1 = -k_1 sign(s_P) \\ V_Q^{ref} = V_Q^N + V_Q^{eq} \end{cases} \quad \begin{cases} w_2 = -M_1 \sqrt{|s_P|} sign(s_P) \\ V_Q^N = w_1 + w_2 \end{cases} \quad (18)$

The constants k_i and M_i are chosen in a manner to assure in finite time the convergence of the sliding manifolds as follows [70]:

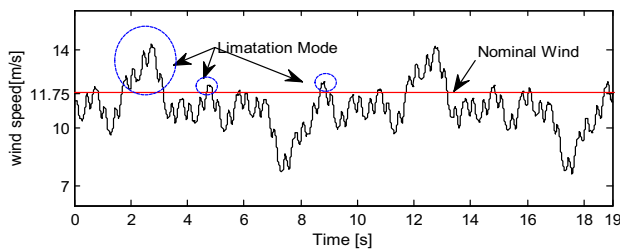


Fig. 11 The wind speed profile in (m/s)

$$\begin{cases} k_i > \frac{\mu_i}{L_g} \\ M_i \geq \frac{\mu_i(k_i + \mu_i)}{L_g^2(k_i - \mu_i)} \\ |G_i| < \mu_i; \quad i = 1, 2 \end{cases}$$

5 Results and discussion

To evaluate this work, the entire wind turbine system and its proposed control system was implemented in the environment “MATLAB/Simulink” which the PMSG/WT parameters are provided in “Appendix”. The simulation tests were carried out under an average wind profile around (11.75 m/s) shown in in Fig. 11.

It is noted that in Fig. 11, at below nominal wind speed (11.75 m/s), the WT operates in tracking mode (region II), the MPPT controller proposed in this paper (FLC–SOSMC–MPPT) ensures the optimum monitoring point of maximum power with high reliability while maintaining the power coef-

ficient to maximum $C_{pmax} = 0.48$ with an optimum value of $\lambda_{opti} = 8.1$ as shown in Fig. 12a, b. Figure 12c, d, represent the instantaneous variation of mechanical power extracted and monitoring of the maximum point around ORC respectively, these figures show the judicious choice of the proposed algorithm which explains high efficiency and flexibility of tracking (follow the MPP) and introduces the best power quality product with a minimal stress and mechanical vibration on the mechanical part (shaft, blade) as represented in Fig. 12d. To protect the WT system above the rated wind speed (region III), a control mode 2nd was applied (power limitation). Consequently the C_p and λ are reduced. The curve shown in Fig. 12c, demonstrating the reliability and the ability to adapt (switching) of the control system in (parts II and III).

As indicated above, the SOSMC algorithm is used for generating a current reference (to the FOClloop) to regulate the speed of PMSG. We can see that in both regions (II and III) of operation, the proposed SOMSC properly follows the speed reference with a negligible error [0.1, -0.1] rad/s as shown in Fig. 13b. To verify the effectiveness of the proposed control approach “SOSMC”, we compared in the same pattern of results with those of FOSMC. The speed control based on FOSMC has an oscillatory response (see Fig. 13a) throughout the simulation, which can cause mechanical vibration, a pulsating torque and poor quality of the extracted mechanical power. However, the SOSMC removes thephenomenon of the chattering, giving a smooth path tracking and a significant decrease of the error of sliding and control effort.

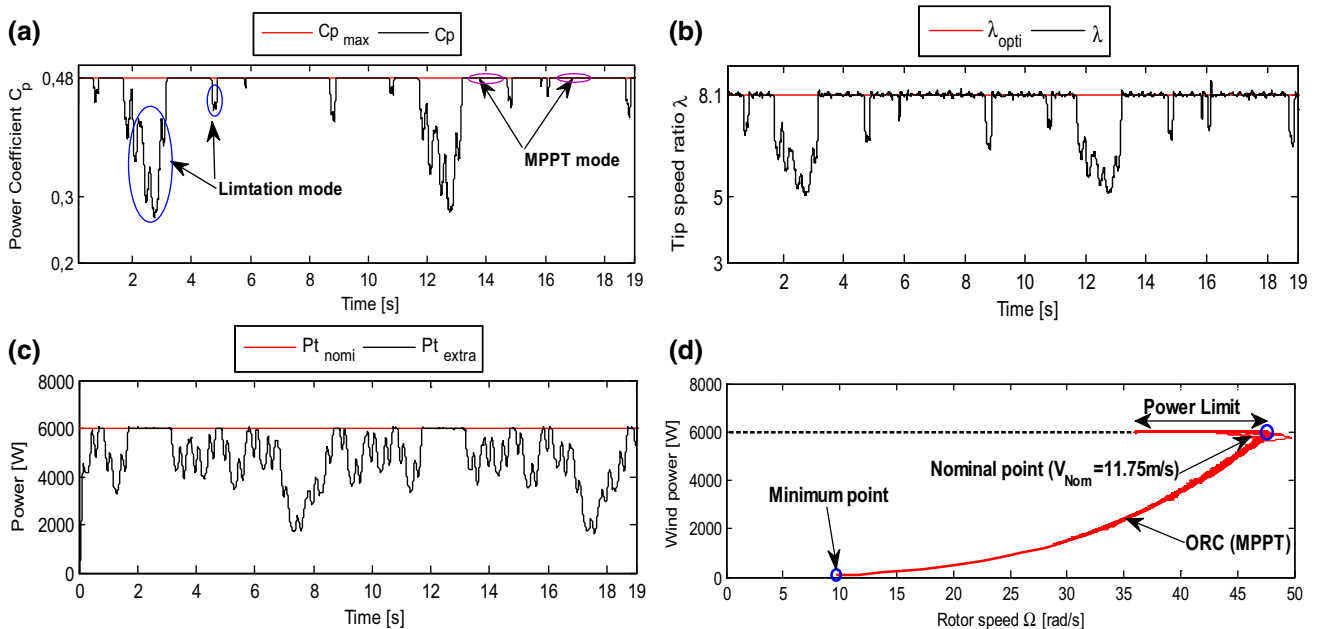


Fig. 12 FLC–SOSMC–MPPT: **a** C_p , **b** λ and **c** the power generation in both region and **d** the real tracking of the optimal rotational speed ORC used in region (II, III)

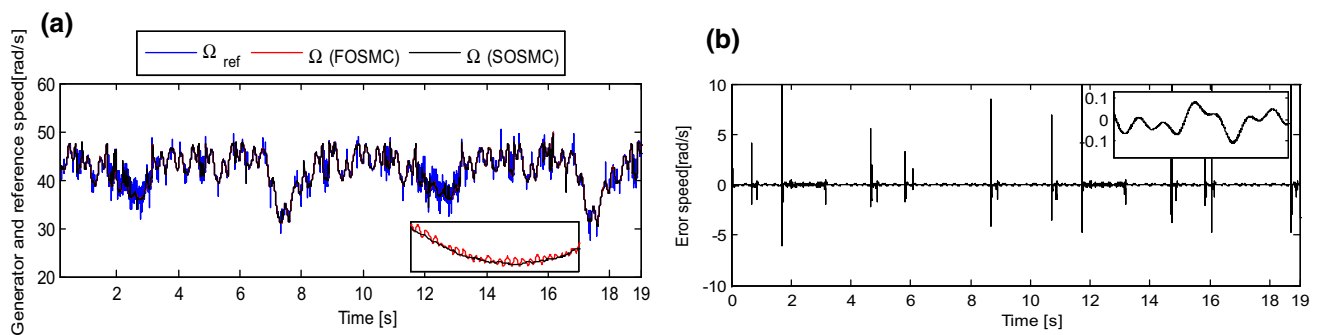


Fig. 13 **a** FOSMC and SOSMC speed control and **b** error speed

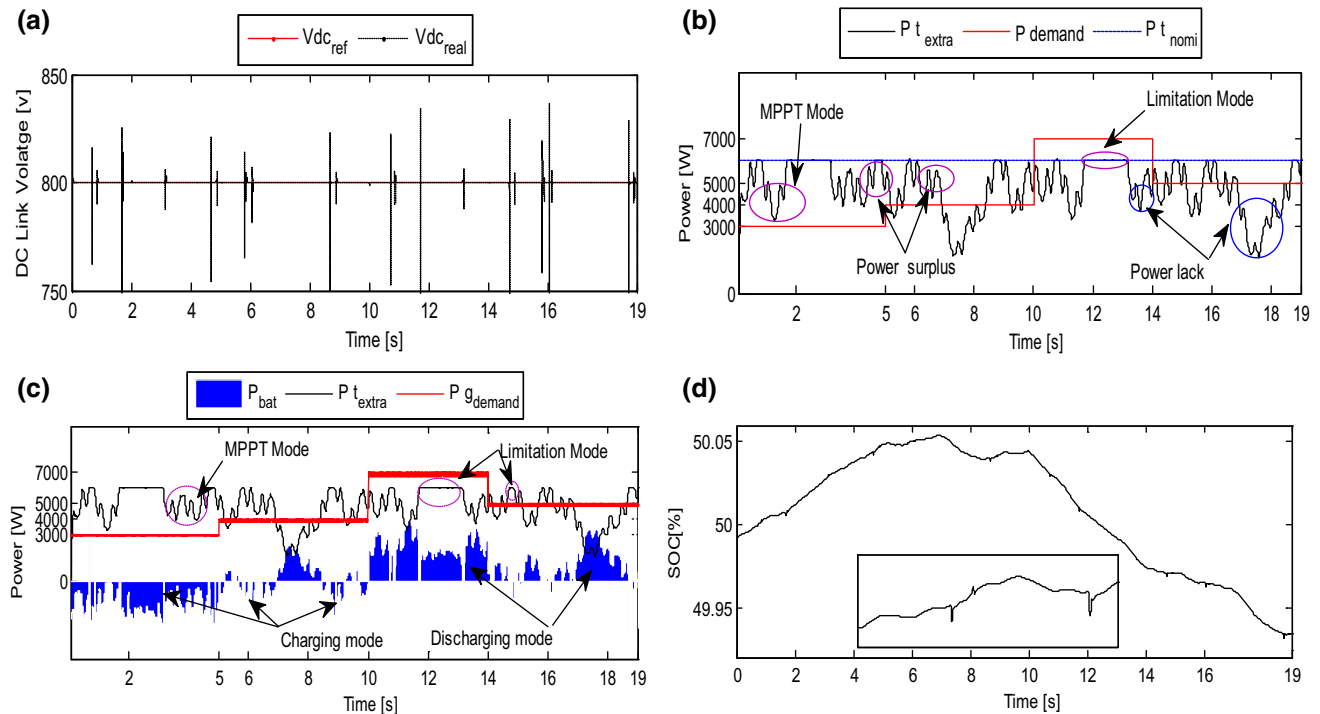


Fig. 14 ESS control: **a** DC link voltage; **b** ‘extracted, nominal, demand’ active power; **c** ‘battery, extracted, grid’ active power and **d** SOC of battery

Whatever the instantaneous variation of the required or available power (from the wind), the exchange of electric power between the PMSG and the grid is assured only if the DC-bus is set at a constant value (nominal). The battery side converter (DC/BESS) is to preserve the DC-link voltage 800 V near its nominal value, as observed in Fig. 14a.

The electric power estimated in diverse sectors of our proposed hybrid system (as well in region II and III, as illustrated in Fig. 14b, c). The desired power ‘reference’ is initially fixed to 3000 W in (5 s). At $t=[5-10\text{ s}]$, the demand is increased to a value up to 4000 W and after she continues to increase to 7000 W during the period of [10–14 s], finally, for the duration of [14–19 s] the power has been decreased to 5000 W as shown in Fig. 14b, c.

- From [0 to 5 s], the electric power demand by the consumer (grid) is $P_{demand} = 3000\text{ W}$ (see Fig. 14b, c). This power (P_{demand}) is inferior to the wind power exist (extracted power at the same time) [$P_{demand} < P_{extra}$]. At this time, a battery charging cycle starts and continues until the SOC reaches 50.048% or more. During recharge, the battery is stored the excess power provided by the PMSG, which makes the storage system in the field of wind energy from an essential feature.
- [5–10 s], it is found that the $P_{demand} = 4000\text{ W}$ (a predefined value) that is “lower or higher” to the wind energy available for conversion (extracting) (Fig. 14b, c). Therefore, can be observed that: in this case, the power recommended by the user (required) is greater than the power generated by the turbine (extracted) [$P_{demand} >$

Table 2 THD current

Controller types	PI (conventional) (%)	FOSMC (%)	PI (fractional) (%)	SOSMC (%)
Current THD	3.96	3.86	0.93	0.59

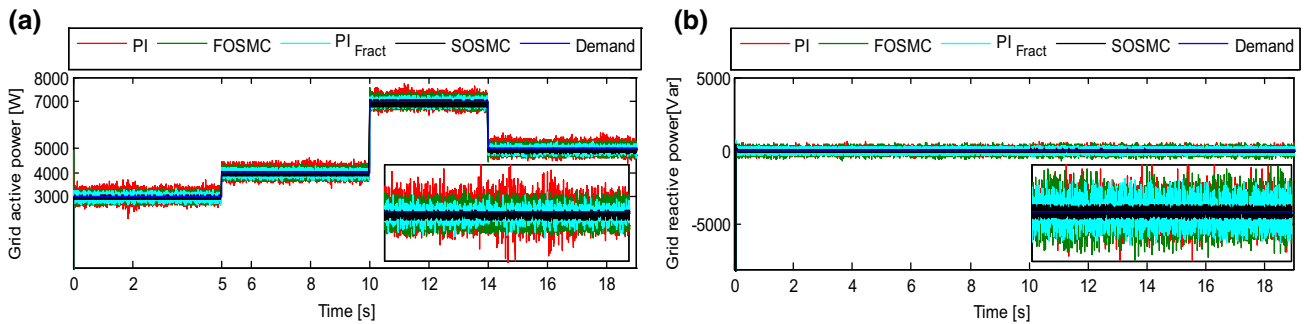


Fig. 15 DPC-SVM (four controllers): **a** grid active power and **b** grid reactive power

P_{extra}]. from which a part of the energy stored in the battery is deflected towards the outlet of PMSG (discharging mode) to compensate the demand deficit accompanied by a decrease of SOCup to 50.03%. Next, under conditions where the consumer need is satisfied and the wind speed is increasing, this leads to an increase of the extracted power compared to the required energy in the connection point (the request) [$P_{extra} > P_{demand}$]. In this case, there’s an excessiveness of the energy produced at the PMSG output and which will be retained (charging mode) in the battery through (DC/DC) with a marked increase in SOS as shown in Fig. 14d.

- The need for the power required by the consumer is increased to 7000W during the period [10–14s], in this period, the wind speed is insufficient [$v_{aver} = 11.5$ m/s] to provide this amount of power (demand) [$P_{demand} > P_{extra}$]. For this reason, a compensation cycle is activated by battery (discharging mode) to cover the lack of the required power. If the wind works in “power limitation mode”. Meanwhile, a battery discharge cycle remains on the same status until 14s and a significant decrease in SOS continues to 49.97% as shown in Fig. 14d.
- The same phenomenon of the interval [5–10s] is identical to the period [14–19s]. During the time interval [14–19s] where the demand for power is 5000W, the latter is inferior or superior to the power derived by the turbine $P_{demand} > P_{extra}$ noted in Fig. 14b, c. In this situation, the ESS battery (delivers/absorbed) electrical energy (discharging/charging) to compensate or store for (absence/surplus) of the power (supplied to the grid/provided by the PMSG). Of the foregoing, it can be affirmed that the hybrid system applied in this work is able to operate in unforeseeable conditions (region II or III) and overcoming diverse constraints, according.

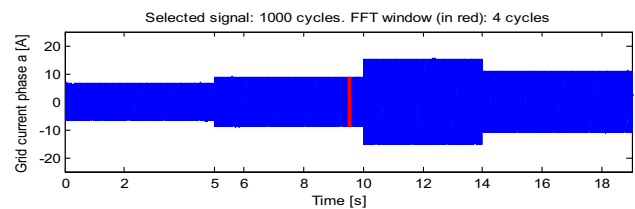


Fig. 16 Grid current phase “A”

After ensuring to provide the energy required by the user (ESS), the quality of this last depends in the control strategies applied to the variables (controllable) related to the grid. For this objective: a new direct power control DPC-SVM used nonlinear control SOSMC has been realized to achieve an effective control to the amount of power grid (active and reactive power). To assess the merit of our choice SOSMC, a comparison was made between four types of controllers ($PI_{conventional}$, $PI_{fractional}$, FOSMC and SOSMC), these results are supported by a harmonic analysis of each regulator as is shown in Table 2.

Figure 15 displays the electrical power injected in the grid, controlled via the proposed DPC-SVM and used four different types of regulators. From Fig. 15a, b, all types of controllers ($PI_{conventional}$, $PI_{fractional}$, FOSMC and SOSMC) can track the desired value precisely. But a clear difference between the various regulators appears at the quality level (flexibility) of the active and reactive power, with a clear priority to the (SOSMC/ $PI_{fractional}$). Simulation results show the superiority of the proposed regulator (SOSMC) based on the algorithm of “super twisting” that guarantees a smooth follow the desired path without chattering phenomenon or oscillations that appear exclusively in the FOSMC. On the other hand, in relation to the two best resulting regulators (SOSMC, $PI_{fractional}$), we have observed the superiority SOSMC with a high efficiency and smooth to track the desired slip trajectory precisely unlike the “ $PI_{fractional}$ ”.

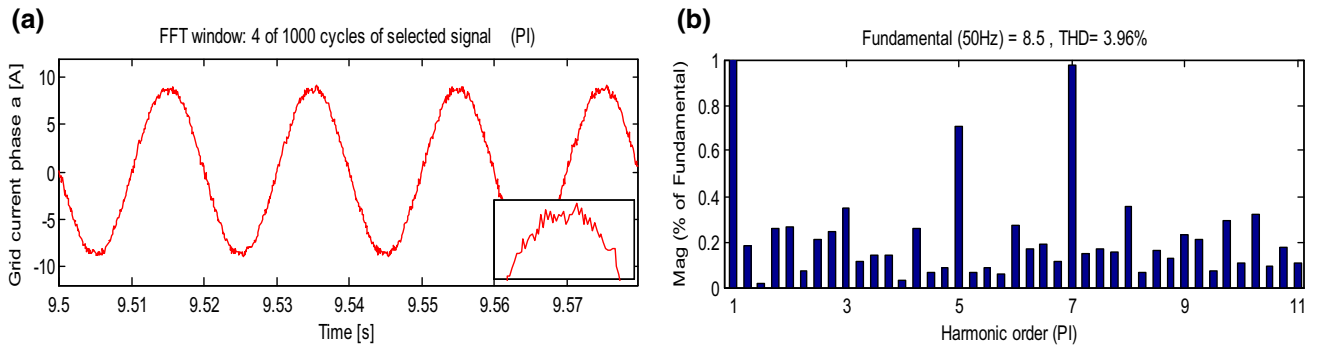


Fig. 17 **a** Grid current for $PI_{conventional}$, **b** THD for $PI_{conventional}$

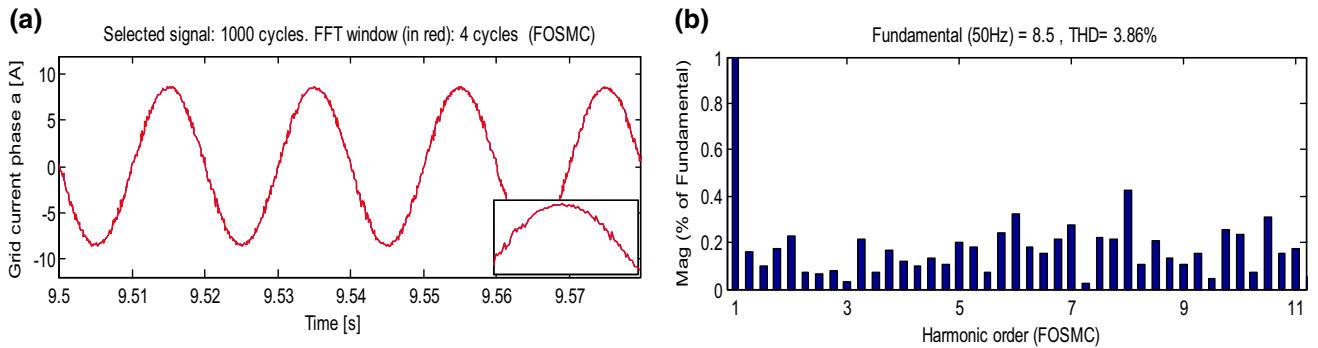


Fig. 18 **a** Grid current for FOSMC, **b** THD for FOSMC

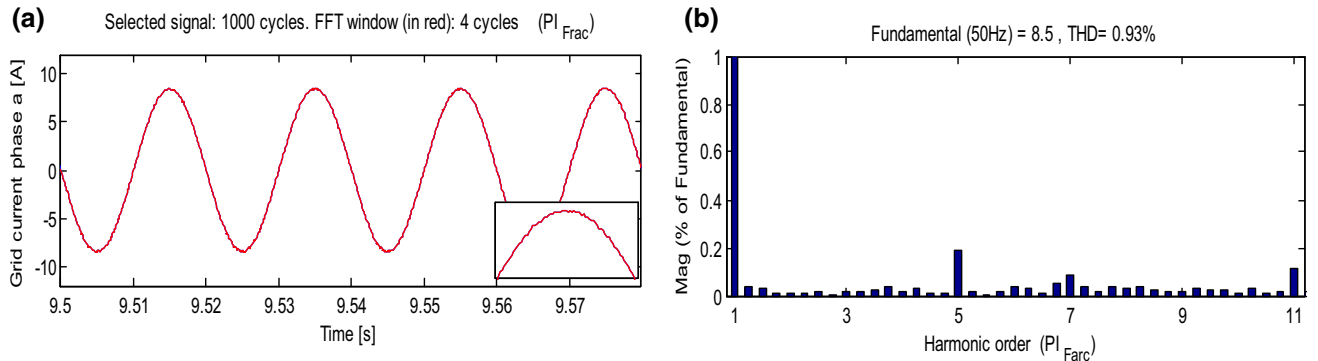


Fig. 19 **a** Grid current for PI_{frac} , **b** THD for $PI_{fractional}$

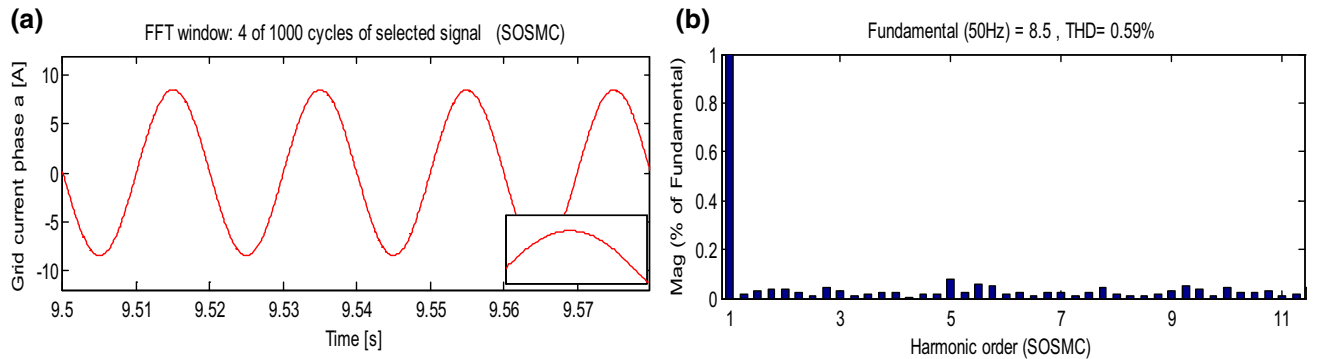


Fig. 20 **a** Grid current for SOSMC, **b** THD for SOSMC

Figure 16 represents the current injected into the phase A in the grid. To clarify the effectiveness of the approach proposed control (DPC–SVM) and the performance of SOSMC used in this technique, we conduct an evaluation and a comparison with (FOSMC– $PI_{\text{conventional}}$ and $PI_{\text{fractional}}$). An analysis of harmonic distortion of each controller was required as is shown in Figs. 17, 18, 19 and 20. The THD of the current (phase A) is displayed in Figs. 17 and 18b are bigger and achieves 3.96 and 3.86% respectively. That means, a distorted form of very undesirable current (phase A) throughout the simulation is observed in Figs. 17 and 18a. We concluded that the use of ($PI_{\text{conventional}}$ /FOSMC) creates a poor quality of the injected grid electrical energy (possibility of degradation of electrical grid). In Figs. 19 and 20b, we noticed a decrease in the best current distortion (0.59 and 0.93%) when we use (SOSMC/ $PI_{\text{fractional}}$) respectively. A significant superiority (SOSMC) is illustrated in the smooth shape of the current (due to the suppression of odd harmonics) as shown in Fig. 20a, b.

A significant improvement was observed in terms of reduction in THD, filtering and removal of odd harmonics [3–11] (with a smooth waveform without distortion). From the above and the result summarized in the Table 2. We conclude that SOSMC method attenuates approximately more than 80 and to 40% of odd harmonics contained in the (FOSMC, $PI_{\text{conventional}}$) and ($PI_{\text{fractional}}$) respectively.

6 Conclusion and future work

In this research, a mathematical model of a hybrid wind turbine was designed and studied. This design is supported by a new supervisory control system and power management in the both areas (II and III). Compared to existing literature, our suggested architecture of control systems (supervisory control) provides to the WTs a freedom to operate in an expanded range with high protection in nominal wind speed. By simulation study, to evaluate our choice, a comparison has been realized between the proposed controller (SOSMC) with conventional control techniques “classic”, the efficiency of the control architecture has been verified. After analyzing the results, It may be concluded: the proposed control structure based on effective nonlinear algorithm (SOSMC, FLC and SVM) and applied in (hybrid/VSWT) makes the conventional system, stable, enhanced, reliable and effective hybrid system with homogeneous protection, guaranteeing the power quality and management in the system in several operating conditions (region II and II), satisfy energy demand in various working conditions (expands area “II, III”).

In the future work, we wish to exploit a wider ESS (high capacity) when the BESS is in a saturation state. In addition, to evaluate this work the experimental results are necessary (test bench). We anticipate also, to implement these control

techniques on several hybrid systems of energy production or in small wind farm with a higher power. Optimizations in untreated point are considered.

Appendix

See Table 3 and 4.

Table 3 PMSG parameters

Nominal power	$P = 6 \text{ kw}$
Stator resistance	$R_s = 0.4 \Omega$
Direct and quadrature stator inductance	$L_d = L_q = 8.4 \text{ mH}$
Field flux	$\psi_{fl} = 0.4 \text{ wb}$
Number of pole pairs	$n_p = 12$
Inertia	$J_t = 0.089 \text{ kg m}^2$
Friction	$f = 0.0016 \text{ N m}$

Table 4 Wind turbine parameters

Radius of the turbine	$R_t = 2 \text{ m}$
Volume density of the air	$\rho = 1.225 \text{ kg m}^3$
The pitch angle	$\beta = 0^\circ$
Specific optimal speed	$\lambda_{\text{opti}} = 8.1$
Coefficient of maximum power	$C_{p\text{max}} = 0.48$

References

- Nikolova S, Causevski A, Al-Salaymeh A (2013) Optimal operation of conventional power plants in power system with integrated renewable energy sources. *Energy Convers Manag* 65:697–703
- Zou Y, Elbuluk ME, Sozer Y (2013) Simulation comparisons and implementation of induction generator wind power systems. *IEEE Trans Ind Appl* 49(3):1119–1128
- Carranza O, Figueres E, Garcerá G, Gonzalez-Medina R (2013) Analysis of the control structure of wind energy generation systems based on a permanent magnet synchronous generator. *Appl Energy* 103:522–538
- Aissaoui AG, Tahour A, Essounbouli N, Nollet F, Abid M, Chergui MI (2013) A fuzzy-PI control to extract an optimal power from wind turbine. *Energy Convers Manag* 65:688–696
- Abdullah MA, Yatim AHM, Tan CW et al (2012) A review of maximum power point tracking algorithms for wind energy systems. *Renew Sustain Energy Rev* 16(5):3220–3227
- Jaramillo-Lopez F, Kenne G, Francoise Lamnabhi-Lagarigue (2016) A novel online training neural network-based algorithm for wind speed estimation and adaptive control of PMSG wind turbine system for maximum power extraction. *Renew Energy* 86:38–48
- Syed IM, Venkatesh B, Wu B, Nassif AB (2012) Two-layer control scheme for a supercapacitor energy storage system coupled to a doubly fed induction generator. *Electr Power Syst Res* 86:76–83

8. Domínguez-García JL, Gomis-Bellmunt O, Bianchi FD, Sumper A (2012) Power oscillation damping supported by wind power: a review. *Renew Sustain Energy Rev* 16(7):4994–5006
9. Zhao H, Wu Q, Hu S, Xu H, Rasmussen CN (2015) Review of energy storage system for wind power integration support. *Appl Energy* 137:545–553
10. Azar AT, Zhu Q (2015) *Advances and applications in sliding mode control systems*. Springer, Berlin
11. Abdeddaim S, Betka A (2013) Optimal tracking and robust power control of the DFIG wind turbine. *Int J Electr Power Energy Syst* 49:234–242
12. Gao R, Gao Z (2016) Pitch control for wind turbine systems using optimization, estimation and compensation. *Renew Energy* 91:501–515
13. Kumar A, Verma V (2016) Photovoltaic-grid hybrid power fed pump drive operation for curbing the intermittency in PV power generation with grid side limited power conditioning. *Int J Electr Power Energy Syst* 82:409–419
14. Yin X, Lin Y, Li W et al (2015) Adaptive sliding mode backstepping pitch angle control of a variable-displacement pump controlled pitch system for wind turbines. *ISA Trans* 58:629–634
15. Saravanakumar R, Jena D (2015a) Validation of an integral sliding mode control for optimal control of a three blade variable speed variable pitch wind turbine. *Int J Electr Power Energy Syst* 69:421–429
16. Kim H, Son J, Lee J (2011) A high-speed sliding-mode observer for the sensorless speed control of a PMSM. *IEEE Trans Ind Electron* 58(9):4069–4077
17. Ramesh T, Panda AK, Kumar SS (2015) Type-2 fuzzy logic control based MRAS speed estimator for speed sensorless direct torque and flux control of an induction motor drive. *ISA Trans* 57:262–275
18. Thirusakthimurugan P, Dananjayan P (2007) A novel robust speed controller scheme for PMBLDC motor. *ISA Trans* 46(4):471–477
19. Pichan M, Rastegar H, Monfared M (2013) Two fuzzy-based direct power control strategies for doubly-fed induction generators in wind energy conversion systems. *Energy* 51:154–162
20. Li H, Jiahui Wang, Lam H et al (2016) Adaptive sliding mode control for interval type-2 fuzzy systems. *IEEE Trans Syst Man Cybern Syst* 46(12):1654–1663
21. Li H, Wang J, Shi P (2016) Output-feedback based sliding mode control for fuzzy systems with actuator saturation. *IEEE Trans Fuzzy Syst* 24(6):1282–1293
22. Uhlen K, Foss BA, Gjørsæter OB (1994) Robust control and analysis of a wind-diesel hybrid power plant. *IEEE Trans Energy Convers* 9(4):701–708
23. Evangelista C, Valenciaga F, Puleston P (2013) Active and reactive power control for wind turbine based on a MIMO 2-sliding mode algorithm with variable gains. *IEEE Trans Energy Convers* 28(3):682–689
24. Li H, Gao H, Shi P et al (2014) Fault-tolerant control of Markovian jump stochastic systems via the augmented sliding mode observer approach. *Automatica* 50(7):1825–1834
25. Li H, Shi P, Yao D et al (2016) Observer-based adaptive sliding mode control for nonlinear Markovian jump systems. *Automatica* 64:133–142
26. Meghni B, Dib D, Azar AT (2016) A second-order sliding mode and fuzzy logic control to optimal energy management in wind turbine with battery storage. *Neural Comput Appl* 1–18. doi:10.1007/s00521-015-2161-z
27. Assareh E, Biglari M (2015) A novel approach to capture the maximum power from variable speed wind turbines using PI controller, RBF neural network and GSA evolutionary algorithm. *Renew Sustain Energy Rev* 51:1023–1037
28. Witczak P, Patan K, Witczak M, Puig V, Korbicz J (2015) A neural network-based robust unknown input observer design: application to wind turbine. *IFAC Pap OnLine* 48(21):263–270
29. Ata R (2015) Artificial neural networks applications in wind energy systems: a review. *Renew Sustain Energy Rev* 49:534
30. Suganthi L, Iniyan S, Samuel AA (2015) Applications of fuzzy logic in renewable energy systems—a review. *Renew Sustain Energy Rev* 48:585–607
31. Banerjee A, Mukherjee V, Ghoshal SP (2014) Intelligent fuzzy-based reactive power compensation of an isolated hybrid power system. *Int J Electr Power Energy Syst* 57:164–177
32. Castillo O, Melin P (2014) A review on interval type-2 fuzzy logic applications in intelligent control. *Inf Sci* 279:615–631
33. Mérida J, Aguilar LT, Dávila J (2014) Analysis and synthesis of sliding mode control for large scale variable speed wind turbine for power optimization. *Renew Energy* 71:715–728
34. Hong C-M, Huang C-H, Cheng F-S (2014) Sliding mode control for variable-speed wind turbine generation systems using artificial neural network. *Energy Procedia* 61:1626–1629
35. Benbouzid M, Beltran B, Amirat Y, Yao G, Han J, Mangel H (2014) Second-order sliding mode control for DFIG-based wind turbines fault ride-through capability enhancement. *ISA Trans* 53(3):827–833
36. Liu J, Lin W, Alsaadi F, Hayat T (2015) Nonlinear observer design for PEM fuel cell power systems via second order sliding mode technique. *Neurocomputing* 168:145–151
37. Evangelista CA, Valenciaga F, Puleston P (2012) Multivariable 2-sliding mode control for a wind energy system based on a double fed induction generator. *Int J Hydrogen Energy* 37(13):10070–10075
38. Eltamaly AM, Farh HM (2013) Maximum power extraction from wind energy system based on fuzzy logic control. *Electr Power Syst Res* 97:144–150
39. Meghni B, Saadoun A, Dib D, Amirat Y (2015) Effective MPPT technique and robust power control of the PMSG wind turbine. *IEEJ Trans Electr Electron Eng* 10(6):619–627
40. Sarrías R, Fernández LM, García CA, Jurado F (2012) Coordinate operation of power sources in a doubly-fed induction generator wind turbine/battery hybrid power system. *J Power Sources* 205:354–366
41. Sarrías-Mena R, Fernández-Ramírez LM, García-Vázquez CA, Jurado F (2014) Improving grid integration of wind turbines by using secondary batteries. *Renew Sustain Energy Rev* 34:194–207
42. Sharma P, Sulkowski W, Hoff B (2013) Dynamic stability study of an isolated wind-diesel hybrid power system with wind power generation using IG, PMIG and PMSG: a comparison. *Int J Electr Power Energy Syst* 53:857–866
43. Liu J, Meng H, Hu Y, Lin Z, Wang W (2015) A novel MPPT method for enhancing energy conversion efficiency taking power smoothing into account. *Energy Convers Manag* 101:738–748
44. Nasiri M, Milimonfared J, Fathi SH (2014) Modeling, analysis and comparison of TSR and OTC methods for MPPT and power smoothing in permanent magnet synchronous generator-based wind turbines. *Energy Convers Manag* 86:892–900
45. Daili Y, Gaubert J-P, Rahmani L (2015) Implementation of a new maximum power point tracking control strategy for small wind energy conversion systems without mechanical sensors. *Energy Convers Manag* 97:298–306
46. Kortabarria I, Andreu J, de Alegría IM, Jiménez J, Gárate JI, Robles E (2014) A novel adaptive maximum power point tracking algorithm for small wind turbines. *Renew Energy* 63:785–796
47. Hong C-M, Chen C-H, Tu C-S (2013) Maximum power point tracking-based control algorithm for PMSG wind generation system without mechanical sensors. *Energy Convers Manag* 69:58–67
48. Narayana M, Putrus GA, Jovanovic M, Leung PS, McDonald S (2012) Generic maximum power point tracking controller for small-scale wind turbines. *Renew Energy* 44:72–79
49. Yin M, Li G, Zhou M, Zhao C (2007) Modeling of the wind turbine with a permanent magnet synchronous generator for integration. In *IEEE Power Engineering Society general meeting*, pp 1–6

50. Jain B, Jain S, Nema RK (2015) Control strategies of grid interfaced wind energy conversion system: an overview. *Renew Sustain Energy Rev* 47:983–996
51. Benelghali S, El Hachemi Benbouzid M, Charpentier JF, Ahmed-Ali T, Munteanu I (2011) Experimental validation of a marine current turbine simulator: application to a permanent magnet synchronous generator-based system second-order sliding mode control. *IEEE Trans Ind Electron* 58(1):118–126
52. Rafiq M, Rehman S, Rehman F, Butt QR, Awan I (2012) A second order sliding mode control design of a switched reluctance motor using super twisting algorithm. *Simul Model Pract Theory* 25:106–117
53. Soler J et al (2005) Analog low cost maximum power point tracking PWM circuit for DC loads. In: *Proceedings of the fifth IASTED international conference on power and energy systems*, Benalmadena, Spain, June 15–17
54. Gkavanoudis SI, Demoulias CS (2014) A combined fault ride-through and power smoothing control method for full-converter wind turbines employing supercapacitor energy storage system. *Electr Power Syst Res* 106:62–72
55. Pena R, Cardenas R, Proboste J, Asher G, Clare J (2008) Sensorless control of doubly-fed induction generators using a rotor-current-based MRAS observer. *IEEE Trans Ind Electron* 55(1):330–339
56. Tapia G, Tapia A, Ostolaza JX (2007) Proportional–integral regulator-based approach to wind farm reactive power management for secondary voltage control. *IEEE Trans Energy Convers* 22(2):488–498
57. Azar AT (2012) Overview of type-2 fuzzy logic systems. *Int J Fuzzy Syst Appl* 2(4):1–28
58. Azar AT (2010) *Fuzzy systems*. IN-TECH, Vienna. ISBN: 978-953-7619-92-3
59. Azar AT, Vaidyanathan S (2015) Handbook of research on advanced intelligent control engineering and automation. In: *Advances in computational intelligence and robotics (ACIR) book series*. IGI Global, USA
60. Azar AT, Vaidyanathan S (2015) Computational intelligence applications in modeling and control. In: *Studies in computational intelligence*, vol 575, Springer, Germany
61. Azar AT, Vaidyanathan S (2015) *Chaos modeling and control systems design, studies in computational intelligence*, vol 581. Springer, Berlin
62. Zhu Q, Azar AT (2015) Complex system modelling and control through intelligent soft computations. In: *Studies in fuzziness and soft computing*, vol 319. Springer, Germany
63. Azar AT, Serrano FE (2015) Design and modeling of anti wind up PID controllers. *Complex system modelling and control through intelligent soft computations*. Springer, Berlin, pp 1–44
64. Azar AT, Serrano FE (2015) Adaptive sliding mode control of the Furuta pendulum. In: Azar AT, Zhu Q (eds) *Advances and applications in sliding mode control systems, studies in computational intelligence*, vol 576. Springer, Berlin, pp 1–42. doi:10.1007/978-3-319-11173-5_1
65. Azar AT, Serrano FE (2015) Deadbeat control for multivariable systems with time varying delays. In: Azar AT, Vaidyanathan S (eds) *Chaos modeling and control systems design, studies in computational intelligence*, vol 581. Springer, Berlin, pp 97–132. doi:10.1007/978-3-319-13132-06
66. Mekki H, Boukhetala D, Azar AT (2015) Sliding modes for fault tolerant control. In: Azar AT, Zhu Q (eds) *Advances and applications in sliding mode control systems, studies in computational intelligence book Series*, vol 576. Springer, Berlin, pp 407–433. doi:10.1007/978-3-319-11173-5_15
67. Luo Y, Chen Y (2012) Stabilizing and robust fractional order PI controller synthesis for first order plus time delay systems. *Automatica* 48(9):2159–2167
68. Ebrahimkhani S (2016) Robust fractional order sliding mode control of doubly-fed induction generator (DFIG)-based wind turbines. *ISA Trans* 63:343–354
69. Munteanu I, Bacha S, Bratcu AI, Guiraud J, Roye D (2008) Energy-reliability optimization of wind energy conversion systems by sliding mode control. *IEEE Trans Energy Convers* 23(3):975–985
70. Beltran B, Ahmed-Ali T, Benbouzid MEH (2008) Sliding mode power control of variable-speed wind energy conversion systems. *IEEE Trans Energy Convers* 23(2):551–558